HHS Public Access

Author manuscript

Mod Pathol. Author manuscript; available in PMC 2015 October 01.

Published in final edited form as:

Mod Pathol. 2015 April ; 28(4): 575–586. doi:10.1038/modpathol.2014.139.

BCOR-CCNB3 Fusions Are Frequent in Undifferentiated Sarcomas of Male Children

Tricia L. Peters[1,2,‡], **Vijetha Kumar**[1,2,‡], **Sumanth Polikepahad**[1,2], **Frank Y. Lin**[3,6], **Stephen F. Sarabia**[1,2], **Yu Liang**[7], **Wei-Lien Wang**[7], **Alexander J. Lazar**[7,8], **Harsha Vardhan Doddapaneni**[5], **Hsu Chao**[5], **Donna M. Muzny**[5], **David A. Wheeler**[4,5,6], **M. Fatih Okcu**[3], **Sharon E. Plon**[3,4,5,6], **M. John Hicks**[1,2,3,6], **Dolores López-Terrada**[1,2,3,6], **D. Williams Parsons**[3,4,5,6], and **Angshumoy Roy**[1,2,3,6]

[1]Department of Pathology, Texas Children's Hospital, Baylor College of Medicine, One Baylor Plaza, Houston, TX, 77030, USA

[2]Department of Pathology & Immunology, Baylor College of Medicine, One Baylor Plaza, Houston, TX, 77030, USA

[3]Department of Pediatrics, Baylor College of Medicine, One Baylor Plaza, Houston, TX, 77030, USA

[4]Department of Molecular and Human Genetics, Baylor College of Medicine, One Baylor Plaza, Houston, TX, 77030, USA

[5]Human Genome Sequencing Center, Baylor College of Medicine, One Baylor Plaza, Houston, TX, 77030, USA

[6]Dan L. Duncan Cancer Center, Baylor College of Medicine, One Baylor Plaza, Houston, TX, 77030, USA

[7]Department of Pathology, University of Texas MD Anderson Cancer Center, 1515 Holcombe Blvd, Houston, TX, 77030, USA

[8]Sarcoma Research Center, University of Texas MD Anderson Cancer Center, 1515 Holcombe Blvd, Houston, TX, 77030, USA

Abstract

The *BCOR-CCNB3* fusion gene, resulting from a chromosome X paracentric inversion, was recently described in translocation-negative ‘Ewing-like’ sarcomas arising in bone and soft tissue. Genetic subclassification of undifferentiated unclassified sarcomas may potentially offer markers for reproducible diagnosis and substrates for therapy. Using whole transcriptome paired end RNA sequencing (RNA-seq) we unexpectedly identified *BCOR-CCNB3* fusion transcripts in an

Corresponding Author: Angshumoy Roy, M.D., Ph.D., Assistant Professor, Departments of Pathology & Immunology and Pediatrics, Baylor College of Medicine, Texas Children's Hospital, 1102 Bates Avenue, FC.830, Houston, TX 77030, Phone: + 1 (832) 824-0901, Fax: + 1 (832) 825-1032, aroy@bcm.edu.

‡Equal contributors

Disclosure/Conflict of Interest: The authors report no conflict of interest.

undifferentiated spindle cell sarcoma. RNA-seq results were confirmed through direct RT-PCR of tumor RNA and cloning of the genomic breakpoints from tumor DNA. Five additional undifferentiated sarcomas with *BCOR-CCNB3* fusions were identified in a series of 42 pediatric and adult unclassified sarcomas. Genomic breakpoint analysis demonstrated unique breakpoint locations in each case at the DNA level even though the resulting fusion mRNA was identical in all cases. All patients with *BCOR-CCNB3* sarcoma were males diagnosed in mid-childhood (7-13 years of age). Tumors were equally distributed between axial and extra-axial locations. Five of the six tumors were soft tissue lesions with either predominant spindle cell morphology or spindle cell areas interspersed with ovoid to round cells. CCNB3 immunohistochemistry showed strong nuclear positivity in 5 tumors prior to oncologic therapy, but was patchy to negative in post-treatment tumor samples. An RT-PCR assay developed to detect the fusion transcript in archival formalin-fixed tissue was positive in all 6 cases, with high sensitivity and specificity in both pre- and post-treated samples. This study adds to recent reports on the clinicopathologic spectrum of *BCOR-CCNB3* fusion-positive sarcomas, a newly-emerging entity within the undifferentiated unclassified sarcoma category, and describes a simple RT-PCR assay that in conjunction with CCNB3 immunohistochemistry can be useful in diagnosing these tumors.

Keywords

sarcoma; fusion; undifferentiated; inversion

Introduction

Undifferentiated unclassified sarcomas constitute a group of rare mesenchymal tumors lacking any evident line of differentiation by standard histopathological, immunophenotypic, ultrastructural, or molecular genetic examination.[1-3] Histologically, undifferentiated/unclassified soft tissue sarcomas are further subclassified into spindle cell, round cell, epithelioid, and pleomorphic subsets under current World Health Organization guidelines, but individual morphologic patterns often coexist.[1, 2, 4] This histologic heterogeneity, combined with the absence of a reproducible immunophenotype or specific molecular markers,[1] frequently poses considerable challenges in diagnosis and in predicting clinical behavior.[1-3, 5, 6] Unclassified sarcomas may also rarely arise in bone as a high-grade pleomorphic sarcoma; however, since the discovery of the *EWSR1* (EWS RNA-binding protein 1)-*ETS*(E26) family gene fusions in Ewing sarcoma, unclassified sarcoma of bone is an infrequent diagnosis.

Unlike other sarcoma subtypes, the taxonomy and diagnosis of which have been refined by the increasing recognition of recurrent molecular genetic aberrations, [1, 2, 4] the molecular and genetic drivers of undifferentiated unclassified sarcomas remain largely unknown. One such recurrent cytogenetic alteration seen in a subset of ‘Ewing sarcoma-like’ round cell undifferentiated sarcomas lacking the pathognomonic *EWSR1-ETS* fusions is the t(4;19)(q35;q13) or t(10;19)(q26.3;q13) translocations, both leading to fusion of *CIC* (capicua homolog) with the *DUX4* (double homeobox 4) gene.[7-13] Round cell sarcomas with the *CIC DUX4* fusion may represent a clinically aggressive subset of undifferentiated sarcomas,[8, 13, 14] and although these tumors share transcriptional subprograms with Ewing

sarcoma,[9] distinct immunophenotypic features[15] suggest a discrete pathological entity. Less commonly, the *EWSR1* gene is fused to non-ETS fusion partners (*NFATC2, PATZ1, SP3,* and *SMARCA5*)[16-19] in Ewing-like round cell undifferentiated sarcomas. However, due to the rarity of these diagnoses, it remains unclear if these tumors are simply variants of Ewing sarcoma or merit a separate subgrouping.[1, 14]

More recently, a novel recurrent paracentric inversion on chromosome X resulting in a *BCOR-CCNB3* fusion gene was identified in ∼4% (24/594) of undifferentiated 'Ewing-like' small round cell sarcomas lacking *EWSR1* gene rearrangements.[20] By gene expression profiling, *BCOR-CCNB3* sarcomas appear distinct from Ewing sarcoma. Moreover, expression of the BCOR-CCNB3 fusion protein appears to drive cell proliferation *in vitro*.[20] Recently, a second series of 10 patients with *BCOR-CCNB3* sarcomas was also reported.[21] Tumors harboring the *BCOR-CCNB3* fusion appear to share some clinical and morphological overlap with the Ewing family of tumors, including the frequent occurrence in long bones of adolescents and young adults, but also appear to have differences, including a strong male predilection and a potentially less aggressive clinical course.[20, 21] The identification of a recurrent driver mutation (*BCOR-CCNB3*) and a unique transcriptional profile and immunophenotype[20] in these tumors suggests the emergence of a distinct genetic subgroup of sarcomas that requires further molecular and clinical characterization.

We investigated the prevalence of the *BCOR-CCNB3* fusion in pediatric and adult undifferentiated unclassified sarcomas, using a combination of whole transcriptome paired-end next-generation sequencing (RNA-seq) and directed RT-PCR, and report on the clinical and histopathological characteristics of six patients with sarcomas harboring this fusion gene. We also report on the development of a targeted RT-PCR assay to detect the *BCOR-CCNB3* fusion in clinical formalin-fixed paraffin embedded tumor specimens.

Materials and Methods

A. Case selection

With Institutional Review Board (IRB) approval from Baylor College of Medicine, the Department of Pathology database and consult files at Texas Children's Hospital were searched between 2000-2013 for bone and soft tissue sarcomas with a final diagnosis containing one of the following search terms: undifferentiated sarcoma; small round blue cell tumor; peripheral primitive neuroectodermal tumor and/or Ewing sarcoma-like tumor; spindle cell tumor; and sarcoma, not otherwise specified. Tumors that lacked characteristic sarcoma-associated chromosomal translocations or fusion genes by cytogenetics, FISH and/or RT-PCR (translocation-negative cases) were selected for inclusion in this study. Cases diagnosed as Ewing sarcoma or peripheral primitive neuroectodermal tumor but lacking a pathognomonic *EWSR1* rearrangement were also included. In cases positive for the *BCOR-CCNB3* transcript in post-treated samples, a second search was performed on the entire database to retrieve the pretreatment diagnostic biopsy, if available. Clinical information (including age, sex, tumor site, treatment, and outcome) and laboratory data were obtained if available from the medical record. A total of 42 cases (23 males, 19 females) were identified for the study, consisting of 31 children (<18 years of age) and 11 adults (range 21-77 years). All adult cases in our consult files were originally diagnosed at

the M. D. Anderson Cancer Center. Seven negative controls were also analyzed including six tumors with characteristic molecular genetic aberrations that would not be expected to harbor a *BCOR-CCNB3* fusion: three cases of Ewing sarcoma with pathognomonic *EWSR1* rearrangements, aberrations, one sarcoma with *CIC* gene rearrangement, an alveolar soft part sarcoma with *ASPSCR1-TFE3* fusion, a mucoepidermoid carcinoma with *MECT1-MAML2* fusion and a normal tonsil. Clinical features of all 42 cases are described in Supplementary Table S1. In three cases (T149, T150, and T236), biopsies of local recurrences and/or distant metastasis were available and included for evaluation.

B. RNA-seq

Concurrently with the above study, patients at the Texas Children's Cancer Center are being enrolled in a second IRB-approved protocol for prospective clinical whole exome sequencing. A sub-study of this protocol includes permission to perform other genomic and RNA analyses for gene discovery. Whole-transcriptome RNA sequencing (RNA-seq) was performed using high quality total RNA (RIN>7) extracted from fresh-frozen tissue to prepare strand-specific, poly-A+ RNA-seq libraries for sequencing on the Illumina platform (Illumina Inc., San Diego, CA). Briefly, poly-A+ mRNA was extracted from 1 μg total RNA, followed by fragmentation and first strand cDNA synthesis. The resultant cDNA was end-repaired, A-tailed and ligated with Illumina PE adapters. The libraries were sequenced in paired-end mode (2 × 100-bp reads) on an Illumina HiSeq 2000 platform following amplification on the cBot cluster generation system (Illumina Inc.). On average, over 84 million paired-end reads were generated per sample.

C. Bioinformatics analysis

Detection of fusion genes was performed using two independent programs with different algorithms: TopHat-Fusion[22] and deFuse.[23] When using TopHat-Fusion, the FASTQ files were aligned to the reference human genome (hg19) by TopHat (ver. 2.0.10) with fusion-search option on. TopHat-Fusion employs a special-purpose algorithm for filtering spurious candidate fusions including removing multi-mapped (>2) reads and pseudogenes, requiring split reads to contain 13-bp of sequence flanking both sides of the fusion junction, filtering intra-chromosomal same strand fusion partners within 100 kb, and retaining candidates supported by evenly-distributed reads around junctions that achieve highest scores in a scoring scheme that prefers uniform depth and no gaps or small gaps.[22] Post-filtration, candidates were annotated using RefGene and ensGene reference. For deFuse (ver. 0.6.1) analyses, high quality FASTQ files were subjected to analysis with default options which yielded 969 fusion candidates. Filters to reduce spurious candidates were applied as reported previously.[23] Nominated candidates were further ranked based on location of fusion breakpoints with coding sequence junctions given highest rank.

D. RT-PCR and Sanger sequencing

RNA was extracted from either formalin-fixed, paraffin-embedded tissue using the Ambion Recover All™ Total Nucleic Acid Isolation Kit (Life Technologies, Carlsbad, CA) or fresh frozen tissue using the mirVana™ miRNA Isolation Kit (Life Technologies) following the manufacturer's instructions for total RNA isolation. Reverse transcription was performed on

500 ng of total RNA using Superscript III First Strand Synthesis System (Life Technologies) and PCR was performed with HotStarTaq DNA polymerase (Qiagen, Valencia, CA) using primers (*BCOR* exon 15 – AGGAGCTGTTAGATCTGGTGGA and *CCNB3* exon 5 – GTGGTTTCTCCATAATGTTTGGT) predicted to generate a 171-bp product. Direct Sanger sequencing was performed using BigDye Terminator v3.1 chemistry (Life Technologies, Inc.) on positive cases.

E. Long-range PCR and genomic breakpoint mapping

Genomic DNA was extracted from fresh-frozen tumor tissue using the QIAamp DNA kit (Qiagen Inc.) following the manufacturer's instructions. For amplification of fragments spanning the genomic breakpoints, long-range PCR was performed with primers as published previously[20] using the TaKaRa LA PCR Kit, v2.1 (Clontech Laboratories Inc., Mountain View, CA) and standard conditions. Using the amplified genomic fragment as template, hemi-nested PCR was performed using the *BCOR* exon 15 forward primer and a series of ten *CCNB3* intron 4 reverse primers successively tiled at approximately 1 kb intervals along the entire intron. The smallest hemi-nested product generated was then cloned and/or sequenced, followed by a BLAST analysis to identify the genomic coordinates of the breakpoints. The breakpoint junction sequences in *BCOR* and *CCNB3* were identified using long range PCR and Sanger sequencing. Sequences of breakpoint mapping primers used in long range PCR are listed in Supplementary Table S2.

F. Fluorescence In-Situ Hybridization (FISH)

Bacterial artificial clones (BAC) flanking the *BCOR* (RP11-91I16 and RP11-665O2) and *CCNB3* genes (RP11-58H17 and RP11-576P23) on the X chromosome were obtained from the BACPAC Resources Center (www.bacpac.chori.org) and labeled with Spectrum Green-dUTP and Spectrum Red-dUTP, respectively. Representative sections of formalin-fixed paraffin embedded tissue were deparaffinized, pre-treated at 80°C for 10 minutes, subjected to protease digestion for 3-7 minutes at 37°C, dehydrated, air-dried and hybridized overnight at 37°C to labeled probes followed by washes at 73°C. Slides were evaluated for the appearance of a bicolor doublet or a fused signal using a fusion probe approach.

G. Histology Review and immunohistochemistry

All cases were reviewed for histomorphologic features, including architectural pattern, presence of necrosis, nuclear features, and mitoses. Cases positive for the *BCOR-CCNB3* fusion underwent independent review by three independent soft tissue pathologists (WLW, AJL, and MJH). Representative 4-um thick sections of the diagnostic biopsy and recurrent specimens of the positive cases were stained with a rabbit polyclonal antibody to CCNB3 (clone HPA000496; Sigma-Aldrich Inc.) at a 1:200 dilution.

Results

A. Identification of a *BCOR-CCNB3* fusion transcript by RNA-seq

To identify novel fusion genes in undifferentiated unclassified sarcomas, we performed whole transcriptome paired-end next-generation RNA sequencing (RNA-seq). In an undifferentiated spindle cell sarcoma, not otherwise specified, arising in an 11-year old male

(case T107), RNA-seq analysis generated 82.8 million paired-end purity-filtered reads of which 1,002 split reads were found to span the junction between *BCOR* exon 15 and *CCNB3* exon 5, producing an in-frame chimeric transcript. In addition, 304 high-quality spanning mate-pairs were identified with one read mapping to *BCOR* exon 15 and the mate-pair mapping to *CCNB3* exon 5 (Figure 1). All fusion-supporting RNA-seq reads contained an identical fusion junction.

We confirmed the RNA-seq result for the *BCOR-CCNB3* fusion using specific primers for *BCOR* exon 15 and *CCNB3* exon 5 in RT-PCR experiments to amplify a 171-bp product that on sequencing revealed an in-frame fusion of the second base in the last codon of *BCOR* (hg19; chrX:39,911,366) and the first base of *CCNB3* exon 5 (chrX:50,051,505) (Figure 1). As reported previously,[20] the fusion sequence is compatible with an aberrant splicing event due to activation of a cryptic 'GT' splice donor site encompassing the last codon and the termination codon of *BCOR* (Figure 1). The fusion was not detected by RT-PCR analysis of a patient-matched lymphoblastoid cell line, indicating that it was a somatic (tumor-specific) event. To confirm this observation, we analyzed the genomic breakpoints between *BCOR* and *CCNB3* using long-range PCR experiments (Figure 2). Using previously published primers,[20] long-range PCR amplified a specific product (>12 kb) only from the tumor DNA but not from the patient-matched lymphoblastoid cell line, confirming the somatic nature of the genomic rearrangement. Primer walking using a series of reverse primers tiled on *CCNB3* intron 4 was performed to map the genomic breakpoint on chromosome X at the *BCOR* 3′UTR (chrX:39,910,580) and *CCNB3* intron 4 (chrX:50,039,717) (Figure 2).

B. Prevalence of *BCOR-CCNB3* in undifferentiated unclassified sarcomas in children and adults

Using the RT-PCR assay described above, we assessed the prevalence of the *BCOR-CCNB3* transcript in archived pediatric and adult cases of undifferentiated unclassified sarcomas. In 41 additional sarcoma cases that met the inclusion criteria (see Methods and Supplementary Table S1), RT-PCR on either frozen or formalin-fixed paraffin-embedded specimens (depending on availability) followed by direct sequencing identified an additional 5 cases that were positive for the *BCOR-CCNB3* fusion (Table 1; Figures 1, 2). As in case T107 described above, the chimeric transcript joined the last codon of *BCOR* to exon 5 of *CCNB3* in all cases. Notably, the fusion transcript was also identified in all available subsequent tissue specimens from these patients including local recurrences and distant metastases. RT-PCR for *BCOR-CCNB3* was appropriately negative in seven specimens included as negative controls (see Methods). As described above, long-range PCR was used to characterize the X chromosome breakpoints of the inversions, resulting in amplified genomic fragments of varying sizes and mapping of the breakpoints to unique locations within the *BCOR* 3′ UTR, the *BCOR-MID1IP1* intergenic region, *CCNB3* exon 4 and *CCNB3* intron 4 (Supplementary Table S3; Figure 2d and Supplementary Figure 1). In addition, FISH performed on two *BCOR-CCNB3* positive cases with dual-color probes on chromosome X[20] detected a bicolor doublet in both cases (Figure 2). In total, *BCOR-CCNB3* fusion transcripts were identified in 6 of 42 undifferentiated unclassified sarcomas (14.3%) examined by RNA-seq and RT-PCR.

C. Histopathology of *BCOR-CCNB3* fusion-positive sarcomas

A review of the pre-treatment diagnostic biopsy specimens from the six *BCOR-CCNB3* positive cases showed tumors of variable cellularity (Figure 3). The tumors were comprised of areas with high cellularity alternating with less cellular areas in which discohesive neoplastic cells were embedded, often in an edematous and myxoid stroma containing occasionally angulated thin-walled vessels. The original diagnosis for two tumors was spindle cell sarcoma and spindle cell neoplasm (T107 and T290, respectively); both tumors contained areas with a prominent spindle cell pattern and in the case of T107, were arranged in a vague fascicular architecture. The other *BCOR-CCNB3* positive tumors were composed of tumor cells with variable nuclear features and included spindled, angulated and ovoid cells overlapping with areas of round cell morphology (Figure 3). Tumor cells had scant to moderate amounts of eosinophilic cytoplasm, and irregular nuclear contours. Nuclei were vesicular with finely dispersed chromatin and occasional indistinct to small nucleoli (as in case T290). None of the tumors showed bizarre nuclear pleomorphism that would be more compatible with a diagnosis of undifferentiated pleomorphic sarcoma. Areas of necrosis were seen in three tumors, ranging from focal to 50% of the tumor area. Mitotic activity, except for T290, was often brisk in the pre-treatment tumors (Table 1), with a median of 30 mitoses per 10 high-power fields (range 1-40).

In two cases (T150 and T290), additional pre-treatment resection specimens were available following the diagnostic biopsy, highlighting the variable cellular morphology of these tumors. T150 was originally diagnosed as sarcoma, not otherwise specified on biopsy, but the resection specimen consisted of predominantly ovoid to stellate to epithelioid cells in a myxoid and occasionally collagenous stroma and the tumor was reclassified as consistent with epithelioid fibrosarcoma. T290 was embolized prior to resection, which may have affected the histopathologic features; nevertheless the resection had areas with higher cellularity and mitotic activity (16 per ten high-power fields) compared to the preceding diagnostic biopsy.

Post-treatment samples were available for evaluation in four cases, including 3 relapsed tumor specimens (T149, T150, and T236). In each of the relapsed cases, tumor cell morphology was similar to the corresponding pre-treatment samples (Figure 3). Interestingly, in T107, the resection specimen immediately following treatment showed similar spindle cell morphology as in the diagnostic biopsy, but also showed areas with tumor cells with distinctly larger rounded nuclei (Figure 1c).

Immunohistochemistry performed as part of the diagnostic work-up showed no specific reproducible immunophenotype. CD99 staining was weak to negative in all tumors. Staining for CCNB3, however, showed strong and diffuse nuclear positivity along with patchy cytoplasmic staining in 5 tumors (Figure 4). In one tumor diagnosed in 1993 (T149), the pre-treatment biopsy specimen stained only patchily with the CCNB3 antibody, and the post-treatment specimen was completely negative. In two other cases (T150, T236) with strong CCNB3 staining pretreatment, the post-treatment resection specimens were only patchily positive or negative. In 3 negative controls tested (2 Ewing sarcomas and 1 *CIC*-rearranged

sarcoma), CCNB3 staining was either absent (Figure 4h) or patchy cytoplasmic, although nuclear expression could be focally seen in one Ewing sarcoma (Figure 4i).

D. Clinical features of *BCOR-CCNB3* fusion-positive sarcomas

A review of the clinical features of the six patients identified with *BCOR-CCNB3* sarcoma revealed that all were male, diagnosed in mid childhood (ages 7 to 13 years), and presented with non-metastatic disease (Table 2). Tumors were equally distributed between axial (paraspinal, chest wall, pelvis) and extra-axial (ankle, calcaneus, thigh) locations. Five of 6 cases appeared to be of soft tissue origin without extensive involvement of bone by imaging and gross examination of the resection specimen (when available). Gross total resection was achieved in 4 of 6 patients, including all 3 extra-axial tumors. One patient (T290) with a completely resected tumor transferred care to another institution shortly following surgical resection and details of adjuvant therapy are unavailable. Adjuvant and/or neo-adjuvant therapy was administered to 4 of 5 patients, including chemotherapy and involved-field radiation therapy in 3 patients and chemotherapy alone in 1 patient (Table 2). All three patients with axial tumors received adjuvant chemotherapy and radiation therapy. Adjuvant chemotherapy backbones were diverse, consisting of regimens based on protocols for non-rhabdomyosarcoma soft tissue sarcoma for two patients (ifosfamide and doxorubicin), Ewing sarcoma for one patient (vincristine, dactinomycin, cyclophosphamide, adriamycin, ifosfamide, etoposide), and rhabdomyosarcoma for one patient (vincristine, dactinomycin, cyclophosphamide). At a median follow-up of 63 months (range 3 to 157 months), three patients developed recurrent disease at 9, 25, and 98 months from diagnosis and two subsequently died of progressive disease (Table 2). Both patients who died from progressive disease had undergone a complete resection of an extra-axial tumor with one having received no neoadjuvant or adjuvant therapy and the other having received adjuvant chemotherapy based on an Ewing protocol.

Discussion

Historically, recurrent chromosomal translocations in sarcomas were discovered through conventional karyotyping and FISH. In recent years, the emergence of next-generation genomic sequencing technologies, and in particular RNA-seq, has led to the discovery of previously unrecognized cryptic intra-chromosomal rearrangements (inversions, deletions, segmental duplications) producing novel oncogenic fusion genes in sarcomas,[24-26] including the recent identification of the *BCOR-CCNB3* gene fusion in ‘Ewing-like’ sarcomas in 2012.[20] Since this original description by Pierron et al.,[20] a second series of 10 sarcomas with the *BCOR-CCNB3* fusion in translocation-negative sarcomas has recently been reported.[21] In the present study, we initially used RNA-seq to identify a *BCOR-CCNB3* fusion gene in an unclassified spindle cell sarcoma. This prompted us to screen for additional cases of the *BCOR-CCNB3* fusion in translocation-negative undifferentiated unclassified sarcomas arising in either bone or soft tissue to further characterize the pathology and clinical course of sarcomas harboring this newly discovered fusion gene.

One of the cases in this series (T149) appeared to arise in the calcaneus on imaging. Biopsy of the large soft tissue extension was diagnosed as a peripheral primitive neuroectodermal

tumor in 1993, prior to routine availability of ancillary FISH and molecular diagnostic techniques, and is similar to the majority of *BCOR-CCNB3* positive sarcomas reported by Pierron et al.[20] and Puls et al.[21] This tumor consisted of round to ovoid cells with fine chromatin, but also spindled areas on close examination which would be unusual for conventional Ewing sarcoma/peripheral primitive neuroectodermal tumor and would be more compatible as an atypical variant. However, in contrast to the two published series that reported the majority of cases to be bone tumors, five of the six cases in this series, including the index case (T107), were originally diagnosed as unclassified undifferentiated soft tissue sarcomas (Table 1). The morphologic features of these 5 cases varied from predominantly spindle cell morphology (T107, T290) to cases with ovoid and angulated cells interspersed with areas of spindle cell morphology, a pattern unusual for either classic Ewing sarcoma or the emerging entity of *CIC-DUX4*-positive sarcomas, both of which are characterized by more uniform small round cell morphology. In both T107 and T290, several spindle cell lesions were considered in the differential diagnosis, including synovial sarcoma, dermatofibrosarcoma protuberans, and low-grade fibromyxoid sarcoma; however, these diagnoses were ruled out through molecular testing for the respective fusion transcripts. In fact, independent expert review of T290 led to reclassification of this tumor as an intermediate-grade myofibroblastic sarcoma, and the untreated resection specimen from T150 was diagnosed as an epithelioid fibrosarcoma, further highlighting the frequency of spindle cell morphology in these tumors. Significantly, in the two previously published series,[20,21] between 25 and 50% of cases were described as having a spindle cell histology, including ‘fusiform’ cell sarcoma, malignant peripheral nerve sheath tumor, synovial sarcoma or simply primitive spindle cell sarcomas. Based on these previous reports as well as our data, it is clear that *BCOR-CCNB3* fusion-positive sarcomas can be characterized by spindle cell morphology that can be predominant or focal in distribution intermixed with areas with round or ovoid cells. It is therefore of practical relevance to emphasize that these tumors are not merely ‘Ewing-like’ sarcomas within the small blue round cell bone tumor category,[1, 13, 14] but can present as unclassified undifferentiated spindle cell sarcomas.

Identification of recurrent and specific diagnostic markers is particularly relevant for pathologists attempting to classify undifferentiated sarcomas, a diagnosis of exclusion that is influenced by the availability (or lack thereof) of advanced diagnostic tools such as electron microscopy and molecular genetic testing.[1, 2] Although undifferentiated sarcomas have long been recognized as a heterogeneous group of tumors, the recent application of molecular genetic techniques isfurther refining this category into genetic subgroups.[2, 4] This has led to a steady decline in the proportion of childhood sarcomas diagnosed as undifferentiated unclassified sarcomas,[3, 27] with best estimates being that these tumors comprise ∼5-10% of childhood sarcomas in the Intergroup Rhabdomyosarcoma Study I and II.[28] With the current study, 6 of 42 undifferentiated unclassified sarcomas proved to be BCOR-CCNB3 fusion-positive sarcomas, representing 14% of all undifferentiated unclassified sarcomas in our cohort. It remains critical to attempt further reproducible subclassification of this heterogeneous group to study the clinicopathologic behavior of the different subsets.[2] Although the specificity and clinical utility of CCNB3 immunohistochemistry as a diagnostic tool needs to be more thoroughly investigated, we confirm in this study previous reports proposing the CCNB3 antibody as a potentially useful adjunct tool in diagnosing this

entity,[20, 21] with 5 of 6 pre-treatment cases showing nuclear CCNB3 expressional though staining was patchy in post-treatment samples. We cannot exclude the possibility that the absence of CCNB3 immunopositivity in the one pre-treatment diagnostic biopsy in our series (T149) was due to the age of the formalin-fixed paraffin-embedded tissue block (21 years). Significantly, however, anRT-PCR assay for detecting the *BCOR-CCNB3* fusion in formalin-fixed paraffin-embedded as well as in frozen tumor tissue was able to reproducibly and robustly detect the fusion transcript in all cases (including the formalin-fixed paraffin-embedded block from T149), including recurrent and metastatic tumor samples, even in those with ambiguous or negative CCNB3 immunostaining. RT-PCR for *BCOR-CCNB3* was appropriately negative in six negative controls, suggesting that molecular testing for this fusion can be a highly sensitive and specific diagnostic tool.

Several clinical features of *BCOR-CCNB3* sarcomas appear somewhat distinctive when compared to entities most likely to be in the differential diagnoses of these lesions, including Ewing sarcoma and *CIC-DUX4* positive sarcomas. First, as in previous reports,[20, 21] *BCOR-CCNB3* fusion-positive sarcomas in this series were seen predominantly in older children. At diagnosis, all six positive cases in our series were in children aged 7 to 13 years; taken together with the previously reported cases, these tumors appear to predominantly occur in children and adolescents (87% [35/40] in patients between 6 and 18 years of age), an age distribution more similar to that of classical Ewing sarcoma[1] than *CIC-DUX4* sarcomas (median age 24 years).[13, 14] Second, all six *BCOR-CCNB3* positive cases in our series were males, and together with the cases published to date, 78% of cases (31/40) have now been reported in males (M:F ratio of 3.4:1), a far greater male predominance than in Ewing sarcoma (1.4:1)[1] or *CIC*-rearranged tumors (~1:1).[13] Indeed the prevalence of *BCOR-CCNB3* fusion-positive sarcomas among male children <18 years age in our series is 35.3% (6/17), a remarkably high frequency for this genetic subgroup among translocation-negative undifferentiated unclassified sarcomas within this patient demographic. A high predominance of X chromosome inversions arising in the male germline and resulting in hemophilia A has been hypothesized to be related to the inability of the single X chromosome in males to use the homologous X chromosome as a template for recombination-mediated repair during meiosis.[29] It is unclear if a similar mechanism exists for mitotic recombination in somatic cells. Third, *BCOR-CCNB3* sarcomas appear to arise in either bone or soft tissue, similar to Ewing sarcoma/peripheral primitive neuroectodermal tumor but distinct from *CIC-DUX4* positive sarcomas, which have been exclusively reported in soft tissues.[7, 8, 13, 14]

The clinical outcomes for patients with *BCOR-CCNB3* are currently unclear, given the small number of such patients reported to date and the heterogeneity of treatment regimens administered. Previous reports have described survival as not significantly different than for patients with Ewing sarcoma,[21] which is broadly consistent with the outcomes observed in the current series. Although none of our six *BCOR-CCNB3* positive patients were observed to have metastatic disease at diagnosis, of the four patients followed for more than one year, 3 have recurred (at 9, 25, and 98 months from diagnosis) and 2 have died of disease (at 34 and 157 months). Of note, both of the patients who died initially underwent a total resection of an extra axial tumor. On the other hand, both patients for whom subtotal resections were

initially achieved are alive without evidence of disease at 93 and 94 months following diagnosis, including one patient (T236) whose tumor recurred at 25 months. Identification of additional cases is necessary before any definitive assessment can be made regarding the clinical behavior of *BCOR-CCNB3* fusion-positive sarcomas.

The pathogenic role of *BCOR-CCNB3* fusions in sarcomas remains to be determined. Whereas CCNB3 is thought to be a meiotic cyclin restricted to spermatocytes, the *BCOR* gene, originally discovered to encode a nuclear corepressor of BCL6, regulates mesenchymal stem cell function through epigenetic modification of histone methylation.[30] The expression of the *BCOR-CCNB3* fusion gene in undifferentiated unclassified sarcomas is therefore consistent with the presumed activity of the BCOR promoter in putative mesenchymal progenitor cells. Given that the entire BCOR protein is part of the putative fusion oncoprotein, further studies are needed to investigate the specific role of the different domains in BCOR. Remarkably for a fusion gene partner, BCOR has been identified as both the N-terminal partner (*BCOR-RARA* in acute promyelocytic leukemia[31]) as well as the C-terminal partner (*ZC3H7B-BCOR* in endometrial stromal sarcoma[32] and ossifying fibromyxoid tumor[33]) in different cancers suggesting alternate mechanisms for oncogenesis in these tumors.

The practical utility of subclassifying undifferentiated/unclassified tumors into genetic subgroups lies in appropriate risk-stratification and development of therapeutic approaches targeted towards the specific fusion transcripts and/or downstream signaling pathways regulated by the fusion gene. This report adds to the growing body of evidence that *BCOR-CCNB3* sarcomas are predominantly seen in male children, and suggest that this diagnosis be strongly considered in males diagnosed with translocation-negative undifferentiated unclassified spindle cell sarcomas and not only tumors with Ewing-like morphology. Routine molecular diagnosis of this entity using RT-PCR either alone, or in combination with CCNB3 immunohistochemistry, is the most reproducible diagnostic approach for these tumors and would provide additional cases for future studies to determine risk-stratification, outcome and targeted therapy.

Supplementary Material

Refer to Web version on PubMed Central for supplementary material.

Acknowledgments

The authors acknowledge Angela Major and E. Faith Hollingsworth for technical assistance. The studies were supported by Dan L. Duncan Cancer Center Multi-Investigator Pilot Project, NHGRI/NCI 1U01HG006485 and the Cancer Prevention & Research Institute of Texas (CPRIT) RP120685.

References

1. Fletcher, CDM.; Chibon, F.; Mertens, F. WHO classification of tumours of soft tissue and bone. In: Fletcher, CDM.; Bridge, JA.; Hogendoorn, PCW.; Mertens, F., editors. Undifferentiated/unclassified sarcomas. 4th. IARC; Lyon: 2013. p. 235-8.
2. Fletcher CD. Undifferentiated sarcomas: what to do? And does it matter? A surgical pathology perspective. Ultrastruct Pathol. 2008; 32:31–6. [PubMed: 18446665]

3. Alaggio R, Bisogno G, Rosato A, Ninfo V, Coffin CM. Undifferentiated sarcoma: does it exist? A clinicopathologic study of 7 pediatric cases and review of literature. Hum Pathol. 2009; 40:1600–10. [PubMed: 19647855]

4. Fletcher CD. The evolving classification of soft tissue tumours - an update based on the new 2013 WHO classification. Histopathology. 2014; 64:2–11. [PubMed: 24164390]

5. Pawel BR, Hamoudi AB, Asmar L, et al. Undifferentiated sarcomas of children: pathology and clinical behavior--an Intergroup Rhabdomyosarcoma study. Med Pediatr Oncol. 1997; 29:170–80. [PubMed: 9212841]

6. Somers GR, Gupta AA, Doria AS, et al. Pediatric undifferentiated sarcoma of the soft tissues: a clinicopathologic study. Pediatr Dev Pathol. 2006; 9:132–42. [PubMed: 16822084]

7. Graham C, Chilton-MacNeill S, Zielenska M, Somers GR. The CIC-DUX4 fusion transcript is present in a subgroup of pediatric primitive round cell sarcomas. Hum Pathol. 2012; 43:180–9. [PubMed: 21813156]

8. Italiano A, Sung YS, Zhang L, et al. High prevalence of CIC fusion with doublehomeobox (DUX4) transcription factors in EWSR1-negative undifferentiated small blue round cell sarcomas. Genes Chromosomes Cancer. 2012; 51:207–18. [PubMed: 22072439]

9. Kawamura-Saito M, Yamazaki Y, Kaneko K, et al. Fusion between CIC and DUX4 upregulates PEA3 family genes in Ewing-like sarcomas with t(4;19)(q35;q13) translocation. Hum Mol Genet. 2006; 15:2125–37. [PubMed: 16717057]

10. Rakheja D, Goldman S, Wilson KS, et al. Translocation (4;19)(q35;q13.1)-associated primitive round cell sarcoma: report of a case and review of the literature. Pediatr Dev Pathol. 2008; 11:239–44. [PubMed: 17990934]

11. Somers GR, Shago M, Zielenska M, Chan HS, Ngan BY. Primary subcutaneous primitive neuroectodermal tumor with aggressive behavior and an unusual karyotype: case report. Pediatr Dev Pathol. 2004; 7:538–45. [PubMed: 15547779]

12. Yoshimoto M, Graham C, Chilton-MacNeill S, et al. Detailed cytogenetic and array analysis of pediatric primitive sarcomas reveals a recurrent CIC-DUX4 fusion gene event. Cancer Genet Cytogenet. 2009; 195:1–11. [PubMed: 19837261]

13. Choi EY, Thomas DG, McHugh JB, et al. Undifferentiated small round cell sarcoma with t(4;19)(q35;q13.1) CIC-DUX4 fusion: a novel highly aggressive soft tissue tumor with distinctive histopathology. Am J Surg Pathol. 2013; 37:1379–86. [PubMed: 23887164]

14. Antonescu C. Round cell sarcomas beyond Ewing: emerging entities. Histopathology. 2014; 64:26–37. [PubMed: 24215322]

15. Specht K, Sung YS, Zhang L. Distinct transcriptional signature and immunoprofile of CIC-DUX4 fusion-positive round cell tumors compared to EWSR1-rearranged ewing sarcomas: Further evidence toward distinct pathologic entities. Genes Chromosomes Cancer. 2014

16. Wang L, Bhargava R, Zheng T, et al. Undifferentiated small round cell sarcomas with rare EWS gene fusions: identification of a novel EWS-SP3 fusion and of additional cases with the EWS-ETV1 and EWS-FEV fusions. J Mol Diagn. 2007; 9:498–509. [PubMed: 17690209]

17. Sumegi J, Nishio J, Nelson M, et al. A novel t(4;22)(q31;q12) produces an EWSR1-SMARCA5 fusion in extraskeletal Ewing sarcoma/primitive neuroectodermal tumor. Mod Pathol. 2011; 24:333–42. [PubMed: 21113140]

18. Szuhai K, Ijszenga M, de Jong D, et al. The NFATc2 gene is involved in a novel cloned translocation in a Ewing sarcoma variant that couples its function in immunology to oncology. Clin Cancer Res. 2009; 15:2259–68. [PubMed: 19318479]

19. Mastrangelo T, Modena P, Tornielli S, et al. A novel zinc finger gene is fused to EWS in small round cell tumor. Oncogene. 2000; 19:3799–804. [PubMed: 10949935]

20. Pierron G, Tirode F, Lucchesi C, et al. A new subtype of bone sarcoma defined by BCOR-CCNB3 gene fusion. Nat Genet. 2012; 44:461–6. [PubMed: 22387997]

21. Puls F, Niblett A, Marland G. BCOR-CCNB3 (Ewing-like) Sarcoma: A Clinicopathologic Analysis of 10 Cases, In Comparison With Conventional Ewing Sarcoma. Am J Surg Pathol. 2014

22. Kim D, Salzberg SL. TopHat-Fusion: an algorithm for discovery of novel fusion transcripts. Genome biology. 2011; 12:R72. [PubMed: 21835007]

23. McPherson A, Hormozdiari F, Zayed A, et al. deFuse: an algorithm for gene fusion discovery in tumor RNA-Seq data. PLoS Comput Biol. 2011; 7:e1001138. [PubMed: 21625565]
24. Antonescu CR, Le Loarer F, Mosquera JM, et al. Novel YAP1-TFE3 fusion defines a distinct subset of epithelioid hemangioendothelioma. Genes Chromosomes Cancer. 2013; 52:775–84. [PubMed: 23737213]
25. Lee CH, Ou WB, Marino-Enriquez A, et al. 14-3-3 fusion oncogenes in high-grade endometrial stromal sarcoma. Proc Natl Acad Sci U S A. 2012; 109:929–34. [PubMed: 22223660]
26. Robinson DR, Wu YM, Kalyana-Sundaram S. Identification of recurrent NAB2-STAT6 gene fusions in solitary fibrous tumor by integrative sequencing. Nat Genet. 2013
27. Stein-Wexler R. Pediatric soft tissue sarcomas. Semin Ultrasound CT MR. 2011; 32:470–88. [PubMed: 21963167]
28. Newton WA Jr, Soule EH, Hamoudi AB, et al. Histopathology of childhood sarcomas, Intergroup Rhabdomyosarcoma Studies I and II: clinicopathologic correlation. J Clin Oncol. 1988; 6:67–75. [PubMed: 3275751]
29. Rossiter JP, Young M, Kimberland ML, et al. Factor VIII gene inversions causing severe hemophilia A originate almost exclusively in male germ cells. Hum Mol Genet. 1994; 3:1035–9. [PubMed: 7981669]
30. Fan Z, Yamaza T, Lee JS, et al. BCOR regulates mesenchymal stem cell function by epigenetic mechanisms. Nat Cell Biol. 2009; 11:1002–9. [PubMed: 19578371]
31. Yamamoto Y, Tsuzuki S, Tsuzuki M, et al. BCOR as a novel fusion partner of retinoic acid receptor alpha in a t(X;17)(p11;q12) variant of acute promyelocytic leukemia. Blood. 2010; 116:4274–83. [PubMed: 20807888]
32. Panagopoulos I, Thorsen J, Gorunova L, et al. Fusion of the ZC3H7B and BCOR genes in endometrial stromal sarcomas carrying an X;22-translocation. Genes Chromosomes Cancer. 2013; 52:610–8. [PubMed: 23580382]
33. Antonescu CR, Sung YS, Chen CL, et al. Novel ZC3H7B-BCOR, MEAF6-PHF1, and EPC1-PHF1 fusions in ossifying fibromyxoid tumors--molecular characterization shows genetic overlap with endometrial stromal sarcoma. Genes Chromosomes Cancer. 2014; 53:183–93. [PubMed: 24285434]

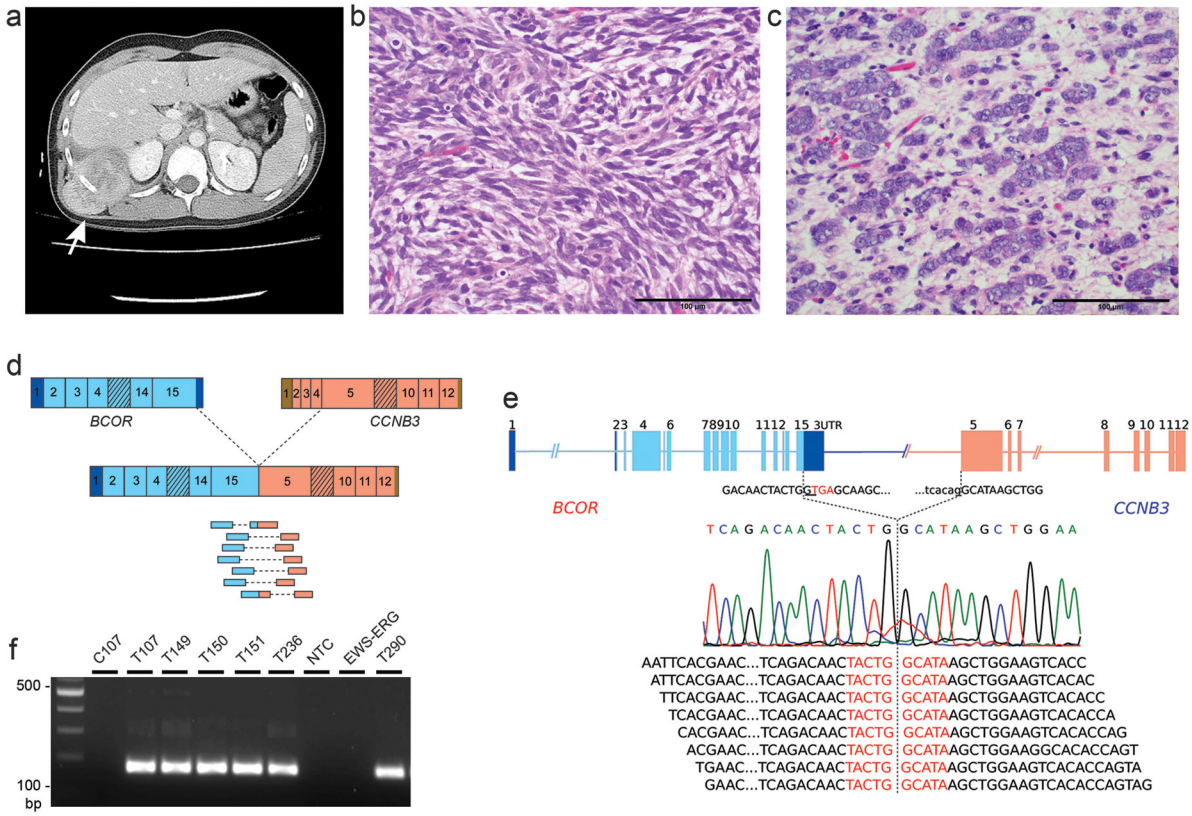

Figure 1.

Identification of the *BCOR-CCNB3* fusion in sarcomas. (a) Axial CT in a 7 year-old male shows a right-sided soft tissue mass (T107) abutting the 9th rib (white arrow). (b) Diagnostic pre-treatment biopsy (b) demonstrating the index case (T107) to be an unclassified spindle cell sarcoma (H&E stain). (c) The post-chemotherapy specimen shows more frequent rounded cells forming nests in a background of edematous to myxoid stroma. (d) Schematic depicting the distribution of paired-end split and spanning RNA-seq reads joining *BCOR* exon 15 with *CCNB3* exon 5. (e) Direct sequencing confirms the RNA-seq reads; the *BCOR-CCNB3* fusion transcript is a result of a cryptic ‘GT’ (underlined) splice donor site activation in BCOR exon 15 leading to skipping of the termination ‘TGA’. (f) RT-PCR with fusion-specific primers shows expression of a 171-bp band only in the tumor (T107) but not in a lymphoblastoid cell line from matched peripheral blood (C107). Additional cases of undifferentiated unclassified sarcoma expressing the *BCOR-CCNB3* fusion (T149, T150, T151, T236, T290), which is not expressed in an Ewing sarcoma with *EWSR1-ERG* translocation (EWS-ERG). NTC, no template control.

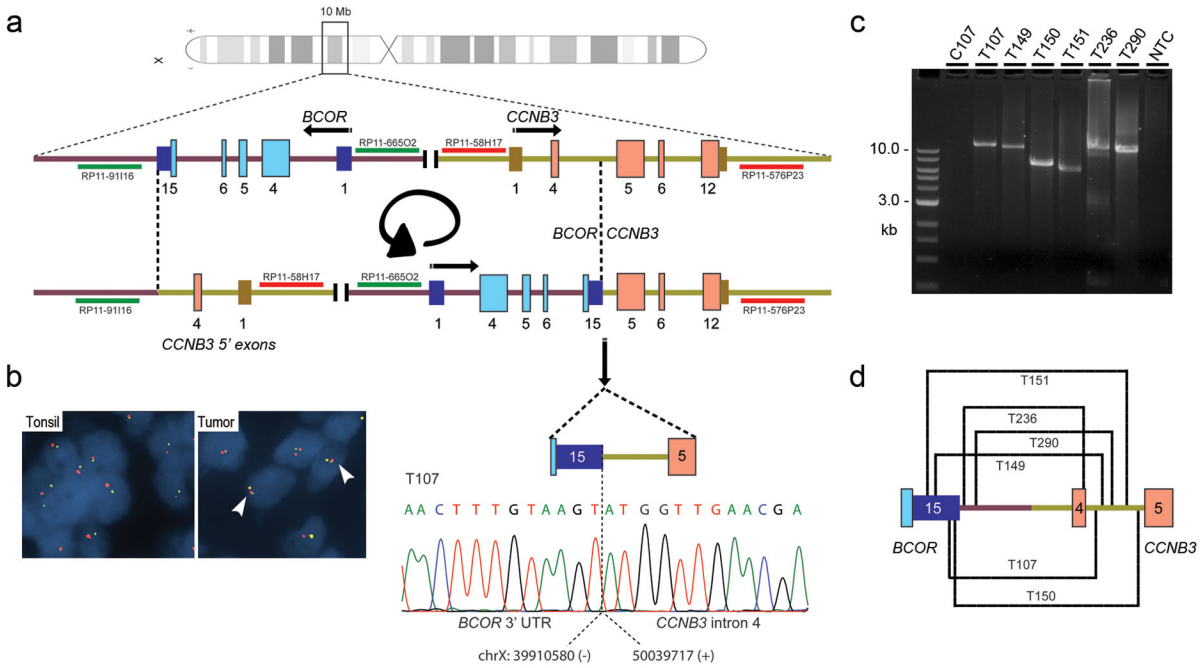

Figure 2.

Genomic rearrangement in *BCOR-CCNB3* sarcomas. (a) Schematic depicting the paracentric inversion on chromosome X. *BCOR* and *CCNB3* are transcribed in opposite directions. The locations of the BACs used for FISH analysis are shown. Dashed lines indicate the genomic breakpoints for the inversions at the *BCOR* 3′UTR or downstream region and in intron 4 of *CCNB3*. The electropherogram depicts the sequence context of the genomic breakpoint in T107. (b) Interphase FISH using probes labeled in Spectrum-Green and Spectrum-Red show two unicolor signals in normal tonsil cells, whereas in *BCOR-CCNB3* sarcoma cells, bicolor doublets (white arrowheads) are seen. (c) Long-range PCR amplification using primers in *BCOR* and *CCNB3* or hemi-nested PCR using *CCNB3* intron 4 primers show specific amplification of genomic DNA fragments of different sizes from all 6 tumors with *BCOR-CCNB3* fusion transcripts, but not from matched lymphoblastoid cell line DNA (C107) for the index case (T107). (d) Schematic depicting the genomic breakpoint locations for the rearrangements in each case.

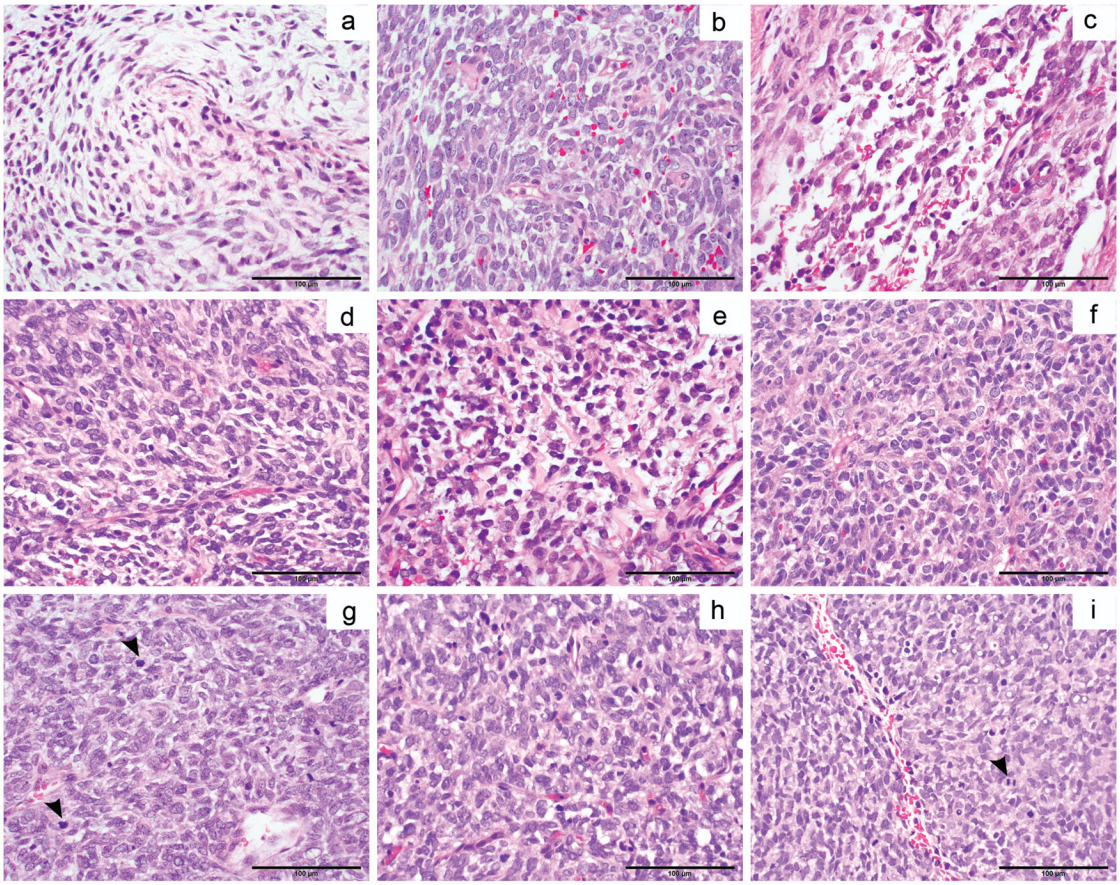

Figure 3.

Histological features of *BCOR-CCNB3* positive sarcomas. (a) and (b) Spindle cell neoplasm (T290) in a myxoid to edematous matrix with more ovoid cells in (b). (c) Undifferentiated sarcoma (T151) with angulated and ovoid cells. (d-f) Pre-treatment (d, e) and the post-treatment relapsed specimen (f) from T150 shows angulated, spindle, and round cells with similar morphology. (g-h) The pre-treatment sample (g) for T149 shows similar features compared to the post-treatment relapse (h) after 8 years off therapy (arrowheads scattered mitoses). (i) T236 with histologic features of undifferentiated sarcoma similar to the other *BCOR-CCNB3* cases. Scale bars, 100 um.

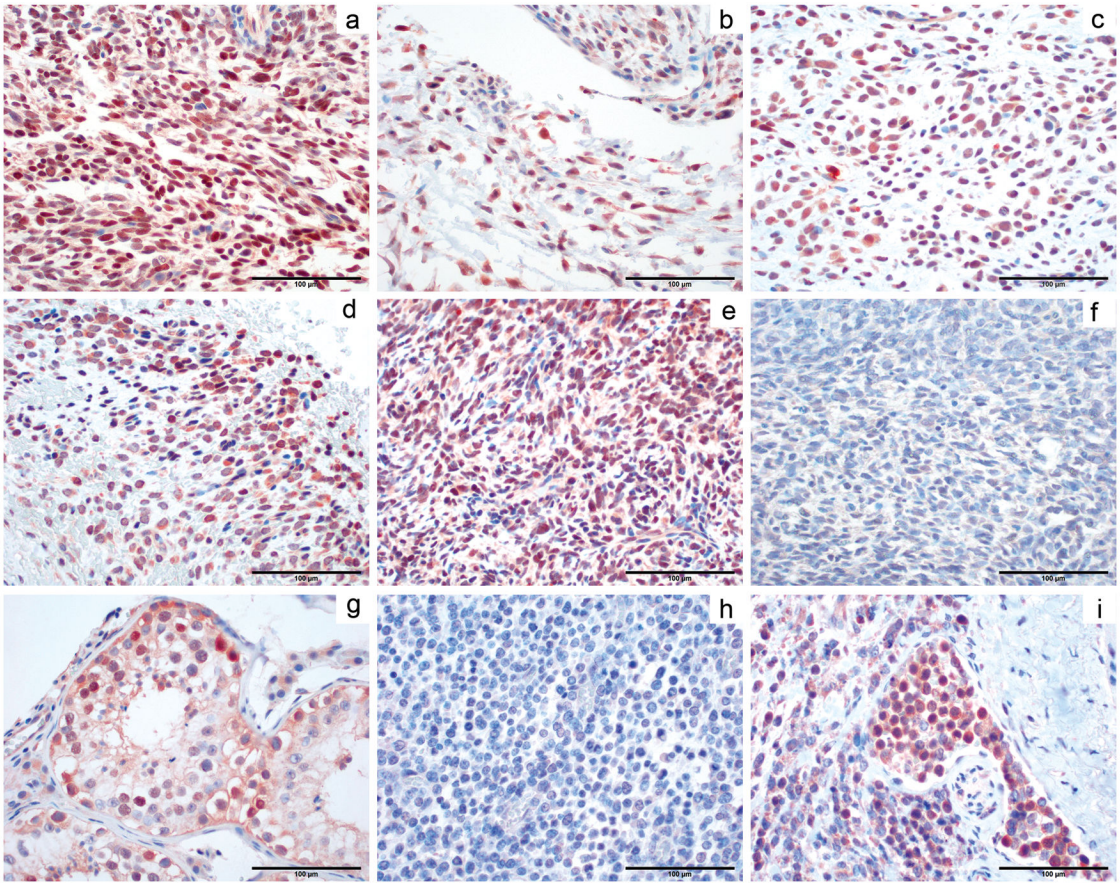

Figure 4.

CCNB3 expression in *BCOR-CCNB3* positive sarcomas. Nuclear CCNB3 immunopositivity is strong and diffuse (a, b, c, and e), strong but patchy (d) and negative in T149 (f). CCNB3 expression in spermatocytes (g) serves as a control. A *CIC*-rearranged small round cell tumor is expectedly negative (h); however, strong patchy nuclear expression is seen in a Ewing sarcoma tumor (i). Scale bars, 100 um.

Table 1

Morphological, immunophenotypic and molecular features of *BCOR-CCNB3* fusion-positive sarcomas

Patient	Tumor site	Histopathology	Mitoses /10 hpf	Necrosis	Immunophenotype	Karyotype	FISH	PCR	Diagnosis	CCNB3 IHC
T107	Soft tissue, chest wall	spindle cells in a storiform pattern with dispersed chromatin and inconspicuous nucleoli	13	Yes	CD117^{+}, fascin^{+}	46,XY	FOXO1^{-}, SYT^{-}, EWSR1^{-}	Neg: COL1A1-PDGFB	Spindle cell sarcoma, NOS	POS
T149	Calcaneus	ovoid cells with finely dispersed chromatin and incospicuous nucleoli	40	No	CD99^{+} (w)	46,XY,t(5;9)(q22;q32)	ND	ND	PNET	NEG
T150	Soft tissue, ankle	small round and spindle cells	16	No	bcl-2^{+}, vim^{+}, CD99^{+} (w)	46,XY	EWSR1^{-}	Neg: EWSR1-FLI1/ERG; SYT-SSX	Sarcoma, NOS	POS
T151	Soft tissue, paraspinal	atypical cells inconspicuous nucleoli	5	No	vim^{+}, CD56^{+}; CD99^{-}	46,XY,inv(9)(p11q12)	ND	ND	Sarcoma, NOS	POS
T236	Pelvis	ovoid to spindle cells with fine chromatin and inconspicuous nucleoli	30	Yes	CD99^{+} (w), vim^{+}	46,XY	ND	Neg: EWSR1-FLI1/ERG; PAX3/7-FOXO1	Undifferentiated sarcoma	POS
T290	Soft tissue,	spindle cells with eosinophilic cytoplasm in a myxoid matrix	1	Yes	CD99^{+} (w), vim^{+}	46,XY	FOXO1^{-}, SYT^{-}, EWSR1^{-}	Neg: FUS-CREB3L1/L2	Spindle cell neoplasm	POS

IHC, immunohistochemistry; vim, vimentin; Neg, negative; NOS, not otherwise specified; PNET, peripheral primitive neuroectodermal tumor; ND, not determined.

Table 2

Clinical features of patients with *BCOR-CCNB3* sarcomas

Patient	Age at diagnosis (years)	Gender	Bone or soft tissue	Site	Anatomic location	Metastatic at diagnosis	Initial resection	Maximum resection	Adjuvant therapy	Chemotherapy backbone	Diagnosis to recurrence (months)	Diagnosis to last contact (months)	Status at last contact
T107	11	M	ST	Axial	Chest Wall	No	Biopsy	GTR	C,X	NRSTS	N/A	11	NED
T149	7	M	Bone	Ext	Calcaneus	No	Biopsy	GTR	C	EWS	98	157	DOD
T150	13	M	ST	Ext	Ankle	No	GTR	GTR	None	N/A	9	34	DOD
T151	10	M	ST	Axial	Paraspinal	No	STR	STR	C,X	NRSTS	N/A	94	NED
T236	10	M	ST	Axial	Pelvis	No	Biopsy	Biopsy	C,X	RMS	25	93	NED
T290	7	M	ST	Ext	Thigh	No	GTR	GTR	ND	ND	N/A	3	NED

M, male; ST, soft tissue; Ext, extra-axial; GTR, gross total resection; STR, subtotal resection; C, chemotherapy, X, radiation therapy, NRSTS, non-rhabdomyosarcoma soft tissue sarcoma chemotherapy with ifosfamide/doxorubicin; EWS, Ewing sarcoma chemotherapy with vincristine, dactinomycin, cyclophosphamide, adriamycin, ifosfamide, etoposide; RMS, rhabdomyosarcoma chemotherapy with vincristine, dactinomycin, cyclophosphamide; N/A, not applicable; DOD, dead of disease, NED, no evidence of disease; ND, not determined. Initial resection denotes extent of surgical resection prior to adjuvant therapy.